

# Guide-Field-mediated Relativistic Reconnection

Pranab J Deka<sup>1,4</sup>, Camille Granier<sup>2,3</sup>, Muni Zhou<sup>4</sup>, Fabio Bacchini<sup>1,5</sup>

<sup>1</sup> Centre for mathematical Plasma Astrophysics, KU Leuven, Belgium

<sup>2</sup> Department of Physics, Stanford University, Stanford, US

<sup>3</sup> Kavli Institute for Particle Astrophysics and Cosmology, Stanford, US

<sup>4</sup> Department of Physics and Astronomy, Dartmouth College, Hanover, US

<sup>5</sup> Royal Belgian Institute for Space Aeronomy, Solar-Terrestrial Centre of Excellence, Belgium

## Introduction

Magnetic reconnection is a leading candidate for powering nonthermal emission in magnetically-dominated astrophysical sources, such as relativistic jets, pulsar winds, and compact-object magnetospheres [2, 3]. In highly-magnetised plasmas ( $\sigma \gtrsim 1$ ), reconnection proceeds rapidly and can produce hard particle spectra extending to very high energies. The resulting nonthermal distributions are set by kinetic-scale physics, as such, particle-in-cell (PIC) simulations have become the primary first-principles tool for this problem.

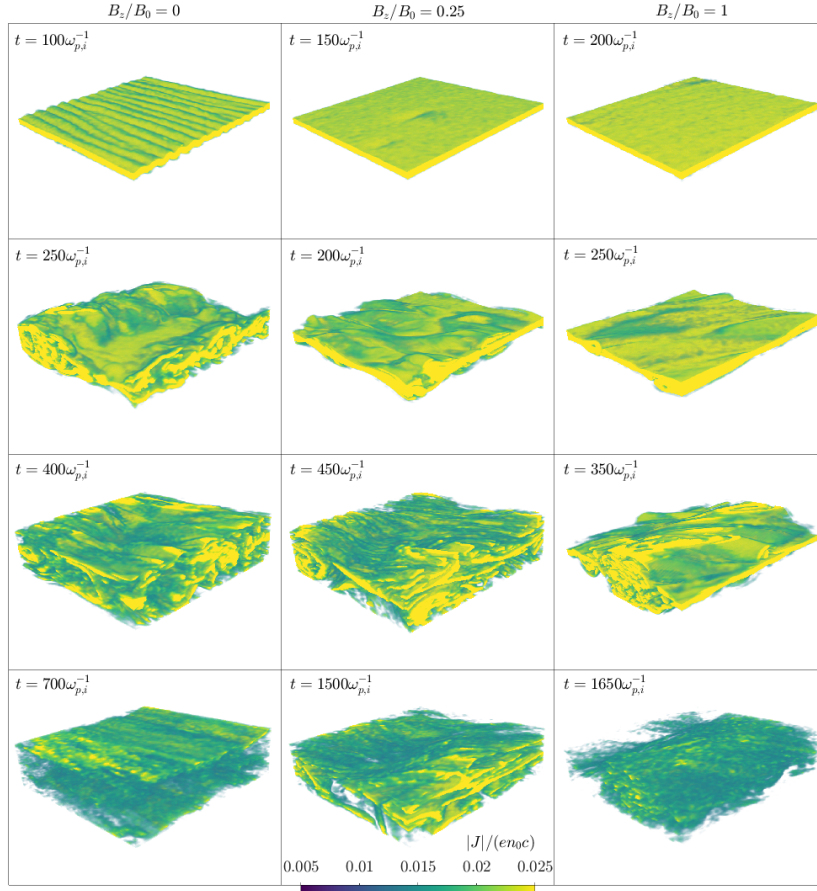


Figure 1: Evolution of the current sheet for  $\sigma_i = 1$  three different guide-field strengths  $B_z/B_0$ .

In three dimensions, the reconnection picture is substantially richer than the 2D plasmoid chain: flux ropes can kink and lose coherence along the current direction, and drift-kink activity can dominate the early evolution, corrugating and broadening the current sheet (Fig. 1) before tearing-mediated reconnection develops [4, 5, 6].

We perform 3D PIC simulations of semirelativistic ion–electron plasma using the iPIC3D code [7] with the Re1SIM algorithm [8]. We initialise a double Harris sheet with the reversing field  $B_x(y)$  supported by a hot drifting Maxwellian and a uniform guide field  $B_z$  along the out-of-plane direction. The upstream plasma follows a Maxwell–Jüttner distribution with a realistic mass ratio  $m_i/m_e = 1836$ . We scan ion magnetisations and guide-field strengths, evolving each case to a quasi-steady state with reconnection seeded purely by PIC noise. Combining magnetic-energy dissipation, Fourier analysis of the tearing and kink modes, current-sheet morphology, and particle energy spectra, we find that the guide-field dependence is non-monotonic: weak guide fields *enhance* reconnection by suppressing the disruptive drift-kink modes that otherwise corrugate and broaden the current sheet, allowing tearing to proceed efficiently, whereas strong guide fields *suppress* it by quenching tearing and reducing the effective outflow speed. The most dissipative cases are therefore not the zero-guide-field runs but those at intermediate  $B_z/B_0$ , where drift-kink disruption is mitigated without impeding tearing [1].

### Magnetic-Energy Dissipation

Reconnection is initiated by the tearing instability, which fragments the thin current sheet into magnetic islands in 2D and flux ropes in 3D. In our configuration, the growth of  $B_y$  (initially zero) serves as a diagnostic of tearing-mode activation, whilst the decay of the reconnecting component  $B_x$  quantifies the conversion of magnetic energy into thermal and nonthermal particle energy. At low magnetisation,  $\sigma_i = 0.1$ , the zero-guide-field case undergoes the strongest decay of  $B_x^2$  and thus the largest total dissipation. Increasing  $B_z/B_0$  monotonically reduces the converted energy, with the strongest guide fields retaining the largest fraction of the initial reconnecting-field energy. Here the guide field acts primarily to stabilise the layer and weaken reconnection. For stronger magnetisations,  $\sigma_i = 1$  and 5, the trend changes qualitatively: a weak but finite guide field can drive *stronger* dissipation than the zero-guide-field case, whereas sufficiently strong guide

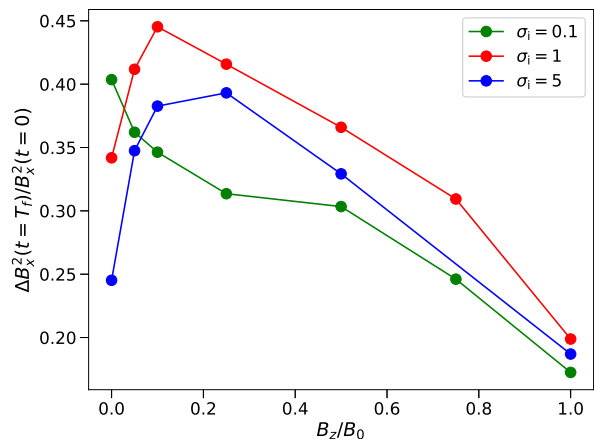


Figure 2: Magnetic-energy dissipation as a function of guide-field strength.

fields again reduce the total conversion. This non-monotonic behaviour is explained as follows: without a guide field, drift-kink activity corrugates and broadens the sheet before tearing fully develops, whereas a weak guide field suppresses this disruptive broadening and allows tearing to proceed efficiently; once the guide field becomes too strong, however, it suppresses tearing and large-scale kink dynamics alike. At  $\sigma_i = 1$  and 5, weak guide fields ( $B_z/B_0 \sim 0.1\text{--}0.25$ ) produce the steepest early-time decline in  $B_x^2$ , indicating a faster reconnection rate than both the zero-guide-field and strong-guide-field cases, and a correspondingly lower final value of  $B_x^2$  that reflects greater total magnetic-energy conversion. The non-monotonic magnetic-energy-dissipation (Fig. 2) trend as a function of guide-field strength indicates an optimal regime in which the guide field is strong enough to mitigate the drift-kink activity, but not strong enough to significantly suppress reconnection or MHD-kink dynamics.

### Tearing vs Drift-Kink vs MHD-Kink Instabilities

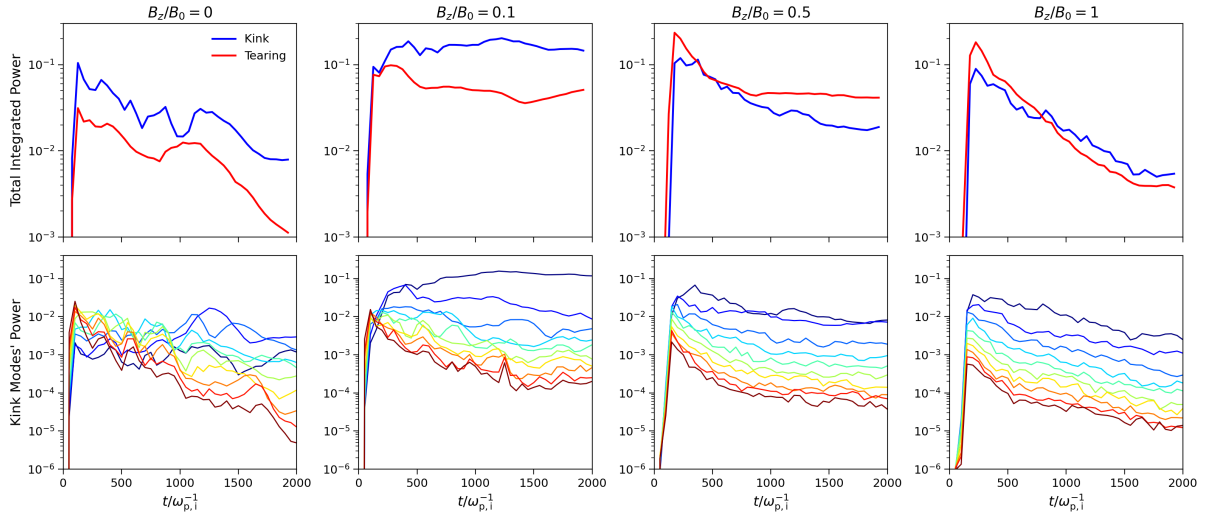


Figure 3: Time evolution of the integrated tearing (red) and kink (blue) power (top panel), and of the first ten kink-like modes (blue to red with increasing  $k$ , bottom panel), for  $\sigma_i = 5$  for different guide-field strengths  $B_z/B_0$ .

To identify which instability controls the evolution of the current sheet, we use the integrated Fourier power in  $B_y$  along  $x$  as a proxy for tearing (red) and that in  $B_x$  along the out-of-plane direction as a proxy for kink-like activity (blue), shown in Fig. 3 for  $\sigma_i = 5$ . In the absence of a guide field, kink activity dominates the early evolution: short-wavelength, high- $k$  drift-kink modes grow on the shortest timescales, typically peaking at  $t \sim 50\text{--}300 \omega_{p,i}^{-1}$ , and corrugate and broaden the current sheet before tearing can fully develop. As the system evolves, the power shifts towards long-wavelength, low- $k$  MHD-like kink distortions that operate on global scales and govern the late-time structure of the sheet.

With the introduction of a weak guide field ( $B_z/B_0 \sim 0.1$ ), the high- $k$  drift-kink modes are preferentially suppressed and their early-time peak delayed and weakened, allowing tearing to develop more effectively and play a larger role in the evolution—the regime that coincides with the enhanced magnetic-energy dissipation. For stronger guide fields ( $B_z/B_0 \gtrsim 0.5$ ), both kink activity and tearing are damped throughout the wave spectrum; the overall evolution becomes smoother and less impulsive, reflecting the reduced efficiency of reconnection in strongly magnetised guide-field configurations. The guide field therefore suppresses the kink channels sequentially, first at small scales and then at large, providing a unified explanation for the non-monotonic dependence of reconnection efficiency on guide-field strength.

## Conclusions

The guide field acts as a key regulator of ion–electron relativistic reconnection: at high magnetisation, weak-to-moderate guide fields enhance magnetic-energy dissipation and nonthermal acceleration by suppressing the disruptive drift-kink modes that broaden the current sheet, whereas strong guide fields suppress reconnection by quenching tearing [1].

## Acknowledgements

PJD acknowledges support from the Research Foundation – Flanders (FWO) via the long stay abroad grant V449025N. FB acknowledges support from the FED-tWIN programme (profile Prf-2020-004, project “ENERGY”), issued by BELSPO, and from the FWO Junior Research Project G020224N granted by the Research Foundation – Flanders (FWO). MZ acknowledges support from the NSF Grant PHY. 2512037. The simulations, for this project, are carried out on the VSC (Belgium), LUMI (Finland), and MeluXina (Luxembourg).

## References

- [1] P. J. Deka, F. Bacchini, M. Zhou, C. Granier, 2026, arXiv:2605.20318 (submitted)
- [2] F. Guo, Y.-H. Liu, S. Zenitani and M. Hoshino, *Space Sci. Rev.* **220**, 43 (2024)
- [3] L. Sironi, D.A. Uzdensky and D. Giannios, *Annu. Rev. Astron. Astrophys.* **63**, 127 (2025)
- [4] G.R. Werner and D.A. Uzdensky, *J. Plasma Phys.* **87**, 905870613 (2021)
- [5] G.R. Werner and D.A. Uzdensky, *Astrophys. J. Lett.* **964**, L21 (2024)
- [6] F. Bacchini, G.R. Werner, C. Granier and J. Vos, *Astrophys. J. Lett.* **991**, L9 (2025)
- [7] S. Markidis, G. Lapenta and Rizwan-uddin, *Math. Comput. Simul.* **80**, 1509 (2010)
- [8] F. Bacchini, *Astrophys. J. Suppl. Ser.* **268**, 60 (2023)